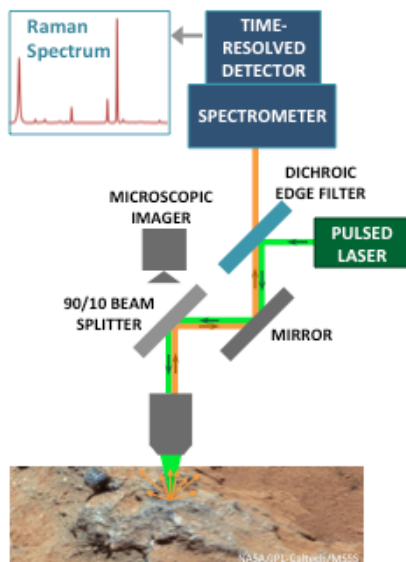


**ADVANCES IN TIME-RESOLVED RAMAN SPECTROSCOPY FOR IN SITU CHARACTERIZATION OF MINERALS AND ORGANICS.** J. Blackberg<sup>1</sup>, E. Alerstam<sup>1</sup>, Y. Maruyama<sup>1</sup>, C. Cochran<sup>1</sup>, G.R. Rossman<sup>2</sup>, <sup>1</sup>Jet Propulsion Laboratory, California Institute of Technology, 4800 Oak Grove Dr., Pasadena, CA 91109, Jordana.blackberg@jpl.nasa.gov, <sup>2</sup>California Institute of Technology, Division of Geological and Planetary Sciences, Pasadena, California 91125, grr@gps.caltech.edu.

**Introduction:** We present recent developments in instrumentation for *in situ* planetary time-resolved Raman spectroscopy, leading to improved performance and identification of both minerals and organics. The Time-Resolved Raman Instrument shown in Figure 1 builds on the widely used 532 nm (green) laser Raman technique, but uses time resolution to detect Raman spectral signatures while eliminating pervasive background interference caused by fluorescence from minerals and organics. The same technique enables operation in daylight conditions without the need for light shielding.



**Figure 1.** High-level schematic of the Time-Resolved Raman Spectrometer, as illustrated for potential mounting on a Rover arm.

By combining capabilities for the identification of minerals present in geological materials, with capabilities to detect organic matter, laser Raman spectroscopy provides a robust *in situ* method for potential future exploration of planetary surfaces [1-5]. Raman is a non-destructive surface technique that requires no sample preparation. Because each band in a Raman spectrum represents interaction of the incident light with a vibrational mode in the crystal, it is highly material specific and can be used for identification and structural characterization of unknown samples. In combination with micro-scale imaging and point mapping, Raman can be used to directly interrogate rocks and regolith materials, while placing compositional

analyses within a microtextural context, essential for understanding surface evolutionary pathways. The addition of time resolution to Raman spectroscopy adds the unique ability to identify and place within context both minerals and organics regardless of background interferences, showing great promise for planetary surface exploration to multiple target bodies identified in the Planetary Science Decadal Survey [6].

The technique takes advantage of the fact that fluorescence can be distinguished from Raman in the time domain. Raman scattering is instantaneous while fluorescence processes are associated with decay times which vary from ps to ms. In natural mixed-phase samples, there can be several fluorescent phases, leading to both long lifetime (mineral) and short lifetime (organic) fluorescence. An illustration of fluorescence rejection using time resolution is shown in Figure 2.

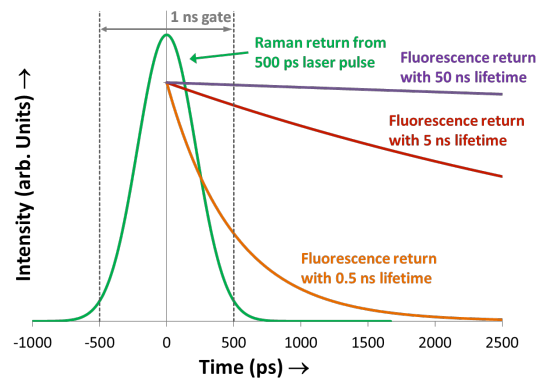


**Figure 2.** Illustration of fluorescence rejection with time-resolved Raman spectroscopy, where only the signal that falls within the chosen time gate is collected. Mineral fluorescence is typically long-lifetime and is easily rejected using a 1 ns gate. Organics present a greater challenge as they often exhibit faster fluorescence lifetimes (ps to ns) as illustrated in the orange and red curves.

**Instrument Overview:** In order to effectively separate Raman from fluorescence background, sub-ns time gating is required. This is accomplished with the use of two essential components: a fast time-resolved detector and a short-pulse laser. Our detector is a custom developed 1024x8 array of Single Photon Avalanche Diodes (SPADs) fabricated using standard silicon CMOS processing, capable of sub-ns time-gating, and operating over a large temperature range without the need for cooling, using very little power [7]. SPADs represent the enabling technology for time-resolved Raman spectroscopy in a miniaturized format [8,9].

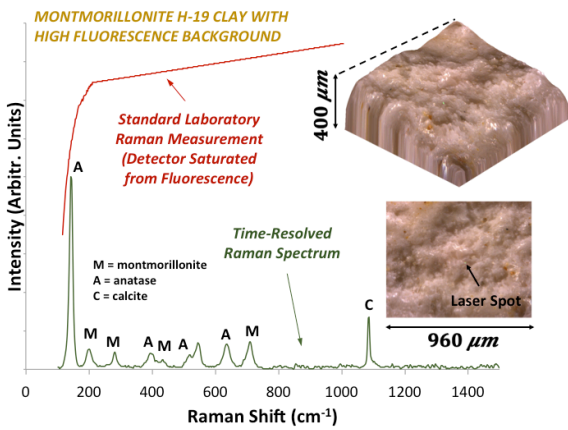


**Figure 3.** Raman spectra showing the benefit of time-resolved Raman for smectite clay, an important class of alteration minerals especially relevant to Mars. The measurement performed on the JPL time-resolved Raman instrument prototype is shown in green and the standard laboratory Raman spectrum measured on a Renishaw spectrometer is shown in red.

SPADs operate in single photon counting mode, with entirely digital output. In the time-resolved Raman spectrometer, the SPAD detector synchronizes with the pulsed laser to collect photons only when the laser pulse is active, thereby rejecting fluorescence and ambient light which can be intense in between laser pulses. In addition to the detector, the need for a short time gate places constraints on the pulsed laser, which must provide a short pulse width as well as a high average power, while keeping the peak power below the sample damage threshold. Our current prototype instrument uses a commercially available 532 nm passively Q-switched microchip laser, operating at 40 kHz repetition rate with  $\sim 600$  ps, 1.5  $\mu$ J pulses. Figure 3 shows the performance capabilities of this instrument, where high background fluorescence is not an impediment to attaining high quality Raman spectra on Mars-analog minerals such as smectite clays.

**Advances in Instrumentation:** Finally, we discuss our most recent advancements for further improving the signal-to-noise performance of the time-resolved Raman instrument. The improved performance is especially notable for dark samples and those containing organics. For example, kerogen and other fossilized biosignatures present a challenge in that they often exhibit short lifetime fluorescence, and they can be dark and thus susceptible to laser damage. The key advancement that promises great improvement in our ability to identify these challenging samples makes use of a new laser technology – high speed microchip (HMC) lasers [10-12]. These are higher repetition rate lasers (MHz) with lower energy per pulse that are currently under development. Raman spectra with our first HMC laser setup show the potential for greatly improved performance as seen in Figure 4.

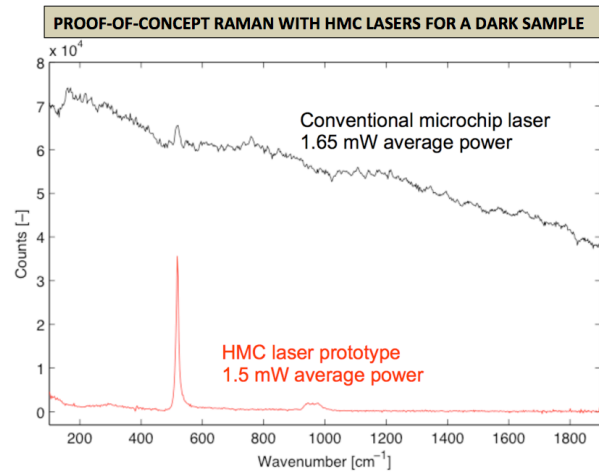


**Figure 4.** Raman spectra of silicon, a typical dark sample, showing the benefits of HMC lasers over conventional microchip lasers. The black curve shows that using our 40 kHz commercial microchip laser, the silicon sample is damaged and the associated broadband plasma emission is visible at 1.65 mW average power ( $\sim 41$  nJ pulse energy). The red curve shows a broadband-free silicon spectrum acquired at almost the same average power, 1.5 mW, with an un-optimized prototype HMC laser setup ( $\sim 650$  kHz rep. rate,  $\sim 180$  ps pulse duration). The lower pulse energy,  $\sim 2.3$  nJ, is below the damage threshold resulting in a clear Raman spectrum. This strategy of moving towards lower pulse energies at higher repetition rates effectively eliminates the sample damage related to the pulsed laser operation, enabling measurements at higher average powers, and ultimately leading to a stronger detected Raman signal.

**Acknowledgements:** The research described here was carried out at the Jet Propulsion Laboratory, California Institute of Technology, under a contract with the National Aeronautics and Space Administration (NASA). Continuous-wave Raman measurements were performed at the Mineral Spectroscopy Laboratory at the California Institute of Technology. SPAD development was performed at Delft University of Technology by the group of Professor Edoardo Charbon.

**References:** [1] D.D. Wynn-Williams et al., *Icarus*, 144, 486-503 (2000), [2] A. Wang, et al. *J. Geophys. Res.*, 108 (E1), 5005 (2003), [3] S.K. Sharma et al. *Spectrochim. Acta Part A*, 68, 1036-1045 (2007), [4] L. Beegle et al., Proceedings of the 11th International GeoRaman Conference 2014 (LPI) #5101, (2014), [5] S.M. Clegg et al., *Applied Spectroscopy*, 68 (9), p. 925-936 (2014), [6] National Academy of Sciences/National Research Council (NRC) Decadal Survey of Planetary Sciences, 2011 [7] Y. Maruyama et al., *IEEE JSSC*, 49 (1) (2014) [8] Blacksberg, U.S. Patent No. 13/925,883, 2013, [9] J. Blacksberg et al. *Optics Letters*, 36 (18), 3672-3674 (2011), [10] A. Steinmetz et al., *Appl Phys B*, 97: 317-320, 2009, [11] E. Mehner et al., *Appl. Phys. B*, 2013, [12] B. Bernard et al., *Proc. SPIE 8960, Laser Resonators, Microresonators, and Beam Control XVI*, 89601D, 2014